

Rotatable Antenna-Enabled Mobile Edge Computing

Qiyao Wang, Beixiong Zheng, Senior Member, IEEE, Xue Xiong, Weidong Mei, Member, IEEE, Changsheng You, Member, IEEE, Qingqing Wu, Senior Member, IEEE, and Jie Tang, Senior Member, IEEE

Abstract—In the evolving landscape of mobile edge computing (MEC), enhancing communication reliability and computation efficiency to support increasingly stringent low-latency services remains a fundamental challenge. Rotatable antenna (RA) is a promising technology that introduces new spatial degrees-of-freedom (DoFs) to tackle this challenge. In this letter, we investigate an RA-enabled MEC system where antenna boresight directions can be independently adjusted to proactively improve wireless channel conditions for latency-critical users. We aim to minimize the maximum computation latency by jointly optimizing the MEC server’s computing resource allocation, receive beamforming, and the deflection angles of all RAs. To address the resulting non-convex problem, we develop an efficient alternating optimization (AO) framework. Specifically, the optimal edge computing resource allocation is derived based on the Karush–Kuhn–Tucker (KKT) conditions. Given the computing resources, the receive beamforming is optimized using semidefinite relaxation (SDR) combined with a bisection search. Furthermore, the RA deflection angles are optimized via fractional programming (FP) and successive convex approximation (SCA). Simulation results verify that the proposed RA-enabled MEC scheme significantly reduces the maximum computation latency compared with conventional benchmark methods.

Index Terms—Rotatable antenna (RA), mobile edge computing (MEC), latency minimization, antenna boresight.

I. Introduction

To meet the ambitious vision of the forthcoming sixth-generation (6G) network featuring ubiquitous connectivity and ultra-low latency, mobile edge computing (MEC) has been widely regarded as a promising technology that offloads computation tasks from resource-limited devices to nearby edge servers, thereby significantly reducing end-to-end latency and energy consumption [1], [2]. However, the performance of MEC systems is fundamentally constrained by the wireless links used for task offloading. The limited coverage, channel capacity constraints, and dynamic network conditions can severely degrade the quality of service (QoS), especially for latency-sensitive applications.

To overcome these challenges, rotatable antenna (RA) technology has recently emerged as an effective approach to enhance spatial degrees of freedom (DoFs) by enabling each antenna to flexibly adjust its three-dimensional (3D) boresight direction [3]–[5]. Unlike conventional fixed antennas, RAs can dynamically reshape their radiation patterns to focus energy toward desired users and suppress interference, thereby improving link reliability and transmission efficiency. As a simplified yet practical member of the movable antenna (MA)/six-dimensional movable antenna

Qiyao Wang and Beixiong Zheng are with the School of Microelectronics, South China University of Technology, Guangzhou 511442, China (e-mails: 202420165372@mail.scut.edu.cn; bxzheng@scut.edu.cn).

Xue Xiong is with the School of Future Technology, South China University of Technology, Guangzhou 511442, China (e-mail: ftxuexiong@mail.scut.edu.cn).

Weidong Mei is with the National Key Laboratory of Science and Technology on Communications, University of Electronic Science and Technology of China, Chengdu 611731, China (e-mail: wmei@uestc.edu.cn).

Changsheng You is with the Department of Electronic and Electrical Engineering, Southern University of Science and Technology, Shenzhen 518055, China, and also with the Shenzhen Key Laboratory of Optoelectronics and Intelligent Sensing, Shenzhen 518055, China (e-mail: youcs@sustech.edu.cn).

Qingqing Wu is with the Department of Electronic Engineering, Shanghai Jiao Tong University, Shanghai 200240, China (e-mail: qingqingwu@sjtu.edu.cn).

Jie Tang is with the School of Electronic and Information Engi-

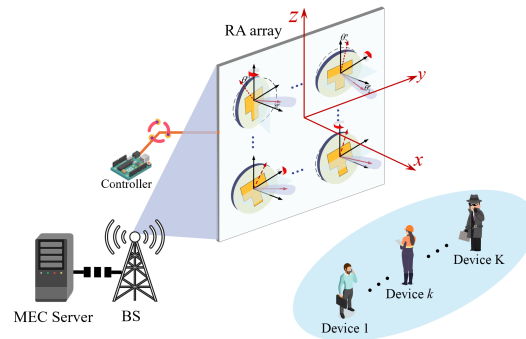


Fig. 1. An RA-enabled MEC system.

(6DMA) family [6], [7], which preserves only rotational flexibility, RA offers a compact and low-cost solution suitable for edge deployments. Owing to these advantages, RA technology has demonstrated notable performance gains in various wireless communication scenarios, such as physical layer security [8], integrated sensing and communication (ISAC) [9], beam-squint mitigation [10], and efficient channel estimation [11]. In particular, by flexibly adjusting the antenna boresight directions, RA can strengthen the wireless links of bottleneck users and mitigate unfavorable channel conditions, thereby making it particularly suitable for latency-sensitive MEC systems. By improving the reliability and quality of the offloading links, RA further enables more adaptive and task-aware scheduling decisions in MEC systems, thereby significantly enhancing the overall computation efficiency and responsiveness. Nevertheless, despite these promising advantages, the integration of RA technology into MEC architectures remains largely unexplored. In particular, how to jointly exploit RA directional control, wireless signal processing, and edge computing resource allocation to minimize computation latency remains an open problem.

Motivated by the above, in this letter we study an RA-enabled MEC uplink communication system, where an RA array is deployed at the base station (BS) to flexibly adjust antenna boresight directions toward different users, as illustrated in Fig. 1. To minimize the maximum computation latency, we formulate a joint optimization problem by optimizing the MEC server’s computing resource allocation, the receive beamforming vectors, and the RAs’ deflection angles. To solve the resulting non-convex problem, we develop an alternating optimization (AO) framework, where the computing resource allocation subproblem is solved via the Karush–Kuhn–Tucker (KKT) conditions and the receive beamforming is optimized through semidefinite relaxation (SDR) and the bisection method, while the RA’s deflection angle subproblem is handled using fractional programming (FP) and successive convex approximation (SCA) techniques. Simulation results verify that the proposed RA-enabled MEC scheme significantly reduces computation latency as compared to conventional benchmarks.

II. System Model And Problem Formulation

As shown in Fig. 1, we consider an RA-enabled MEC uplink communication system, where the BS is equipped with an edge computing server. Specifically, K devices simultaneously transmit data to the BS and may offload part or all of their computation tasks to the associated MEC server. The BS is equipped with a uniform planar array (UPA) consisting of N directional RAs, while each

Under the three-dimensional (3D) Cartesian coordinate system, we assume that the planar array is placed on the y - z plane with $N \triangleq N_y N_z$, where N_y and N_z denote the numbers of RAs along y - and z -axes, respectively, and the reference orientation/boresight of each RA is assumed to be parallel to the positive x -axis. Let $\mathbf{p}_n \in \mathbb{R}^{3 \times 1}$ and $\mathbf{q}_k \in \mathbb{R}^{3 \times 1}$ be the reference positions of the n -th RA and the k -th device, respectively. The deflection angle vector of the n -th RA is defined as $\boldsymbol{\theta}_n \triangleq [\theta_n^e, \theta_n^a]^T$, $n = 1, \dots, N$, where θ_n^e represents the zenith angle between the boresight direction of the n -th RA and the x -axis, and θ_n^a denotes the azimuth angle between the projection of the boresight vector of RA n onto the y - z plane and the z -axis. Accordingly, the pointing vector of each RA can be defined as $\tilde{\mathbf{f}}(\boldsymbol{\theta}_n) = [\cos(\theta_n^e), \sin(\theta_n^e) \sin(\theta_n^a), \sin(\theta_n^e) \cos(\theta_n^a)]^T$. To account for the antenna boresight adjustment range, the zenith angle of each RA is constrained within a prescribed range, given by $0 \leq \theta_n^e \leq \theta_{\max}$, $\forall n$, where θ_{\max} denotes the maximum allowable zenith angle. For notational convenience in the subsequent analysis, we introduce an auxiliary variable $\tilde{\mathbf{f}}_n \in \mathbb{R}^{3 \times 1}$ to represent RA pointing vector associated with $\boldsymbol{\theta}_n$, i.e., $\tilde{\mathbf{f}}_n = \tilde{\mathbf{f}}(\boldsymbol{\theta}_n)$, with $\|\tilde{\mathbf{f}}_n\| = 1$.

A. Communication Model

We consider an uplink communication model, where the computation offloading of the K devices is performed over a predefined frequency bandwidth B and shares the same time resource. All device-to-BS links are assumed to experience quasi-static flat-fading channels. Accordingly, the channel between device k and RA n can be modeled as

$$h_{k,n}(\tilde{\mathbf{f}}_n) = \sqrt{L(d_{k,n})} g_{k,n}, \quad (1)$$

where $L(d_{k,n}) = \zeta_0 (d_0/d_{k,n})^{\alpha_0}$ represents the large-scale channel power gain, ζ_0 is the channel power gain at the reference distance of $d_0 = 1$ meter (m), α_0 denotes the path loss exponent, and $d_{k,n}$ represents the distance from the k -th device to the n -th RA.

Furthermore, we assume that $g_{k,n}$ follows an independent Rician fading model with Rician factor κ_k , given by

$$g_{k,n} = \sqrt{\frac{\kappa_k}{\kappa_k + 1}} \bar{g}_{k,n} + \sqrt{\frac{1}{\kappa_k + 1}} \tilde{g}_{k,n}, \quad (2)$$

where $\bar{g}_{k,n} = \sqrt{G_{k,n}} e^{-j \frac{2\pi}{\lambda} d_{k,n}}$ represents the line-of-sight (LoS) channel component, $\tilde{g}_{k,n} \sim \mathcal{CN}(0, 1)$ denotes the non-LoS (NLoS) channel component characterized by Rayleigh fading, and λ is the signal wavelength. In addition, $G_{k,n}$ denotes the generic directional radiation pattern for each RA, which can be modeled as [4]

$$G(\epsilon, \phi) = \begin{cases} G_0 \cos^{2p}(\epsilon), & \epsilon \in [0, \pi/2), \phi \in [0, 2\pi), \\ 0, & \text{otherwise,} \end{cases} \quad (3)$$

where ϵ and ϕ are the zenith and azimuth angles of any spatial directions with respect to the RA's boresight direction, G_0 is the maximum gain in the boresight direction (i.e., $\epsilon = 0$) with $G_0 = 2(2p + 1)$ satisfying the law of power conservation, and $p \geq 0$ determines the directivity of antenna. Additionally, $\cos(\epsilon_{k,n}) \triangleq \tilde{\mathbf{f}}_n^T \tilde{\mathbf{q}}_{k,n}$ is the projection between the device k 's direction vector $\tilde{\mathbf{q}}_{k,n} \triangleq \frac{\mathbf{q}_k - \mathbf{p}_n}{\|\mathbf{q}_k - \mathbf{p}_n\|}$ and the pointing vector of RA n .

Let $\mathbf{F} \triangleq [\tilde{\mathbf{f}}_1, \tilde{\mathbf{f}}_2, \dots, \tilde{\mathbf{f}}_N] \in \mathbb{R}^{3 \times N}$ denote the RA deflection matrix. The overall channel from BS to device k is given by

$$\mathbf{h}_k(\mathbf{F}) = [h_{k,1}(\tilde{\mathbf{f}}_1), h_{k,2}(\tilde{\mathbf{f}}_2), \dots, h_{k,N}(\tilde{\mathbf{f}}_N)]^T. \quad (4)$$

Denote the uplink offloading transmit power and transmitted symbol of device k by P_k and s_k , respectively, the received signal at the BS is expressed as

$$\mathbf{y} = \sum_{k=1}^K \mathbf{h}_k(\mathbf{F}) \sqrt{P_k} s_k + \mathbf{n}, \quad (5)$$

where $\mathbf{n} \sim \mathcal{CN}(0, \sigma^2 \mathbf{I}_N)$ represents the additive white Gaussian noise (AWGN) with zero-mean and variance σ^2 . Upon receiving \mathbf{y} , the BS applies a linear receive beamforming vector $\mathbf{w}_k^H \in \mathbb{C}^{1 \times N}$ with $\|\mathbf{w}_k\| = 1$ to extract the signal of device k , i.e.,

$$y_k = \mathbf{w}_k^H \mathbf{h}_k(\mathbf{F}) \sqrt{P_k} s_k + \sum_{j=1, j \neq k}^K \mathbf{w}_k^H \mathbf{h}_j(\mathbf{F}) \sqrt{P_j} s_j + \mathbf{w}_k^H \mathbf{n}. \quad (6)$$

Then, the signal-to-interference-plus-noise ratio (SINR) for decoding the signal from the k -th device is given by

$$\gamma_k(\mathbf{w}_k, \mathbf{F}) = \frac{P_k |\mathbf{w}_k^H \mathbf{h}_k(\mathbf{F})|^2}{\sum_{j=1, j \neq k}^K P_j |\mathbf{w}_k^H \mathbf{h}_j(\mathbf{F})|^2 + \sigma^2}. \quad (7)$$

Accordingly, the maximum achievable computation offloading rate of the k -th device is given by

$$R_k(\mathbf{w}_k, \mathbf{F}) = B \log_2(1 + \gamma_k(\mathbf{w}_k, \mathbf{F})). \quad (8)$$

B. Computing Model

We consider that each device k has a computation task consisting of L_k bits, where processing each bit requires c_k CPU cycles. The task can be divided into two parts: one computed locally at the device and the other offloaded to the edge server.

1) Local Computing: Let ℓ_k (in bits) and f_k^l (in cycle/s) denote the task offloaded to the MEC server and CPU frequency of device k , respectively. Accordingly, the time required for undertaking the local computation is defined as $D_k^l(\ell_k) = (L_k - \ell_k) c_k / f_k^l$.

2) Edge Computing: We assume that the edge computing for the k -th device commences only after all its task bits have been fully offloaded. Specifically, the total latency of edge computing contains two parts: the data transmission time from the device to the BS and the computation time at the MEC server. The MEC server allocates computing resource f_k^e for device k , which satisfies:

$$\sum_{k=1}^K f_k^e \leq F_{\max}, \quad f_k^e \geq 0, \quad \forall k, \quad (9)$$

where F_{\max} denotes the maximum computing capacity of the MEC server. In this work, the size of the computation result is assumed to be sufficiently small, such that we can neglect the feedback delay. Therefore, the overall latency associated with task offloading and edge computing is expressed as $D_k^e(\mathbf{w}_k, \mathbf{F}, \ell_k, f_k^e) = \ell_k / R_k(\mathbf{w}_k, \mathbf{F}) + \ell_k c_k / f_k^e$.

Assuming that each device can perform local computation and task offloading simultaneously, the task completion time is determined by the slower processing branch. Hence, the overall computation latency of device k is given by $D_k(\mathbf{w}_k, \mathbf{F}, \ell_k, f_k^e) = \max\{D_k^l(\ell_k), D_k^e(\mathbf{w}_k, \mathbf{F}, \ell_k, f_k^e)\}$, and the maximum computation latency among all the devices is given by $\tau^{\text{comp}} = \max\{D_k(\mathbf{w}_k, \mathbf{F}, \ell_k, f_k^e), \forall k\}$.

C. Problem Formulation

In this paper, we aim to minimize the maximum computation latency τ^{comp} by jointly optimizing the computation offloaded data size $\boldsymbol{\ell} = [\ell_1, \ell_2, \dots, \ell_K]^T$, the edge computing resource allocation for all devices $\mathbf{f}^e = [f_1^e, f_2^e, \dots, f_K^e]^T$, the BS receive beamforming matrix $\mathbf{W} = [\mathbf{w}_1, \mathbf{w}_2, \dots, \mathbf{w}_K]^T$, and the RA pointing matrix \mathbf{F} . The associated optimization problem can be formulated as

$$(P1) \quad \min_{\boldsymbol{\ell}, \mathbf{f}^e, \mathbf{W}, \mathbf{F}} \tau^{\text{comp}} \quad (10a)$$

$$\text{s.t. } \|\mathbf{w}_k\| = 1, \quad \forall k, \quad (10b)$$

$$0 \leq \arccos(\tilde{\mathbf{f}}_n^T \mathbf{e}_1) \leq \theta_{\max}, \quad \forall n, \quad (10c)$$

$$\|\tilde{\mathbf{f}}_n\| = 1, \quad \forall n, \quad (10d)$$

$$\ell_k \in \{0, 1, \dots, L_k\}, \quad k = 1, 2, \dots, K, \quad (10e)$$

$$\sum_{k=1}^K f_k^e \leq F_{\max}, \quad (10f)$$

$$f_k^e \geq 0, \quad k = 1, 2, \dots, K, \quad (10g)$$

where constraint (10b) imposes the unit-norm constraints on receive beamforming vectors; (10c) specifies the maximum zenith angle that each RA is allowed to adjust and (10d) ensures that $\tilde{\mathbf{f}}_n$ is a unit vector; (10e) ensures that the computation offloaded data size is an integer within the range from 0 to L_k for the k -th device; (10f) and (10g) restrict the range of the edge computing resources allocated to each device. Due to the strong coupling variables and the non-convex constraints, problem (P1) is non-convex and difficult to handle. To solve this problem, we propose an AO algorithm to iteratively optimize the four blocks of variables.

III. Proposed Algorithm For Problem (P1)

In this section, we develop an AO-based algorithm for solving problem (P1), which alternately optimizes computation variables, i.e. $\{\boldsymbol{\ell}, \mathbf{f}^e\}$, and communication variables, i.e. $\{\mathbf{W}, \mathbf{F}\}$ in an iterative manner until convergence. Accordingly, problem (P1) can be decomposed into two tractable subproblems.

A. Joint Optimization of Offloaded Data Size and Edge Computing Resource Allocation

Given the receive beamforming matrix \mathbf{W} and the RAs' pointing matrix \mathbf{F} , problem (P1) can be reduced to

$$(P2) \quad \min_{\boldsymbol{\ell}, \mathbf{f}^e} \tau^{\text{comp}} \quad (11)$$

$$\text{s.t. } (10e), (10f), (10g).$$

Although problem (P2) is simplified, it remains challenging to solve optimally since the variables $\boldsymbol{\ell}$ and \mathbf{f}^e are still coupled in (10e)-(10g). To decouple them, we first fix \mathbf{f}^e and optimize $\boldsymbol{\ell}$. Under this condition, (P2) reduces to a set of single-variable optimization problems with respect to ℓ_k , each of which admits a closed-form solution [12], as given by

$$\ell_k^* = \underset{\hat{\ell}_k \in \{\lfloor \hat{\ell}_k^* \rfloor, \lceil \hat{\ell}_k^* \rceil\}}{\text{argmin}} D_k(\hat{\ell}_k), \quad (12)$$

where $\lfloor \cdot \rfloor$ and $\lceil \cdot \rceil$ represent the floor and ceiling operations, respectively, and $\hat{\ell}_k^*$ is given by

$$\hat{\ell}_k^* = \frac{L_k c_k R_k f_k^e}{f_k^e f_k^l + c_k R_k (f_k^e + f_k^l)}. \quad (13)$$

By substituting $\hat{\ell}_k^*$ into (10a) and introducing the slack variable t_1 , problem (P2) can be transformed into the following problem

$$(P2.1) \quad \min_{\mathbf{f}^e, t_1} t_1 \quad (14a)$$

$$\text{s.t. } \frac{L_k c_k^2 R_k + L_k c_k f_k^e}{f_k^e f_k^l + c_k R_k (f_k^e + f_k^l)} \leq t_1, \quad \forall k, \quad (14b)$$

$$(10f), (10g).$$

It can be verified that problem (P2.1) is convex, since the left-hand side of constraint (14b) is convex with respect to f_k^e , while all other constraints are affine. Therefore, the KKT conditions can be applied to derive the closed-form solution of f_k^e . Due to the min-max latency objective, only the multiplier associated with the bottleneck device is active, while the multipliers of all the other devices equal zero. Without loss of generality, we normalize the active

multiplier to unity. Accordingly, the optimal f_k^e for a given dual variable μ is given in closed form as in [12]

$$f_k^e = \frac{\sqrt{\frac{L_k c_k^3 R_k^2}{\mu} - c_k R_k f_k^l}}{f_k^l + c_k R_k}, \quad k = 1, \dots, K, \quad (15)$$

where μ^* denotes the optimal dual variable and can be found via bisection search within the interval $(\mu_l, \mu_u] = \left(0, \min_k \left(\frac{L_k c_k}{f_k^l}\right)\right)$.

B. Joint Optimization of Receive Beamforming and Pointing Matrix

Given the offloaded data size $\boldsymbol{\ell}$ and the edge computing resource allocation vector \mathbf{f}^e , problem (P1) is reformulated as the following optimization problem for optimizing the receive beamforming matrix \mathbf{W} and the RA pointing matrix \mathbf{F} .

$$(P3) \quad \min_{\mathbf{W}, \mathbf{F}} \tau^{\text{comp}} \quad (16)$$

$$\text{s.t. } (10b), (10c), (10d).$$

As shown in Section III-A, at the optimal solution to problem (P2), $D_k^l = D_k^e$, and thus the objective in (16) can be equivalently expressed solely in terms of the edge computation latency. By replacing D_k with D_k^e , and replacing ℓ_k with the closed-form $\hat{\ell}_k^*$ from (13), problem (P3) reduces to

$$(P3.1) \quad \min_{\mathbf{W}, \mathbf{F}} \max_k \frac{L_k c_k f_k^e}{f_k^e f_k^l + c_k R_k (\mathbf{w}_k, \mathbf{F})(f_k^e + f_k^l)} + \frac{\ell_k c_k}{f_k^e} \quad (17)$$

$$\text{s.t. } (10b), (10c), (10d).$$

Moreover, due to the complicated fractional SINR expression shown in (7), we introduce a set of slack variables t_2 and $\{t_{3,k}\}$ to reformulate problem (P3.1) as

$$(P3.2) \quad \min_{\mathbf{W}, \mathbf{F}, t_2, \{t_{3,k}\}} t_2 \quad (18a)$$

$$\text{s.t. } \frac{\ell_k c_k}{f_k^e} \leq t_{3,k}, \quad \forall k, \quad (18b)$$

$$\frac{L_k c_k f_k^e}{f_k^e f_k^l + c_k R_k (\mathbf{w}_k, \mathbf{F})(f_k^e + f_k^l)} + t_{3,k} \leq t_2, \quad \forall k, \quad (18c)$$

$$R_k \leq B \log_2(1 + \gamma_k), \quad \forall k, \quad (18d)$$

$$\gamma_k \leq \frac{P_k |\mathbf{w}_k^H \mathbf{h}_k(\mathbf{F})|^2}{\sum_{j=1, j \neq k}^K P_j |\mathbf{w}_k^H \mathbf{h}_j(\mathbf{F})|^2 + \sigma^2}, \quad \forall k, \quad (18e)$$

$$(10b), (10c), (10d).$$

Problem (P3.2) is still non-convex due to the coupled variables and the fractional SINR constraint in (18e). To address this issue, we further decompose problem (P3.2) into two subproblems.

1) Receive Beamforming Optimization

Given the pointing matrix \mathbf{F} , the SINR constraints reduce to

$$\gamma_k \leq \frac{P_k |\mathbf{w}_k^H \mathbf{h}_k|^2}{\sum_{j=1, j \neq k}^K P_j |\mathbf{w}_k^H \mathbf{h}_j|^2 + \sigma^2}, \quad \forall k. \quad (19)$$

To facilitate convex reformulation, we define $\mathbf{W}_k = \mathbf{w}_k \mathbf{w}_k^H$, which satisfies $\mathbf{W}_k \succeq \mathbf{0}$ and $\text{rank}(\mathbf{W}_k) = 1$. Note that $|\mathbf{w}_k^H \mathbf{h}_k|^2 = \text{tr}(\mathbf{W}_k \mathbf{H}_k)$ and $|\mathbf{w}_k^H \mathbf{h}_j|^2 = \text{tr}(\mathbf{W}_k \mathbf{H}_j)$, where $\mathbf{H}_k = \mathbf{h}_k \mathbf{h}_k^H$ and $\mathbf{H}_j = \mathbf{h}_j \mathbf{h}_j^H$.

The rank-one constraint is non-convex, we relax it to obtain the following SDR problem:

$$(P3.3) \quad \min_{\mathbf{W}, t_2, \{t_{3,k}\}} t_2 \quad (20a)$$

$$\text{s.t. } \gamma_k \left(\sum_{j=1, j \neq k}^K P_j \text{tr}(\mathbf{W}_k \mathbf{H}_j) + \sigma^2 \right) \leq P_k \text{tr}(\mathbf{W}_k \mathbf{H}_k), \quad \forall k, \quad (20b)$$

$$\text{tr}(\mathbf{W}_k) = 1, \quad \forall k. \quad (20c)$$

$$\mathbf{W}_k \succeq \mathbf{0}, \quad \forall k, \quad (20d)$$

$$(18b), (18c), (18d).$$

It can be verified that problem (P3.3) is a quasi-convex optimization problem with respect to $\{\mathbf{W}_k\}$, which can

be solved via bisection search. Specifically, for any given γ_k , the feasibility problem associated with (P3.3) can be reformulated as a convex semidefinite program (SDP). Although the SDR may result in a high-rank solution, a high-quality rank-one approximation can be recovered using Gaussian randomization, which is then used to obtain the corresponding receive beamforming vectors.

2) Pointing Matrix Optimization

For a given receive beamforming matrix \mathbf{W} , problem (P3.2) can be equivalently expressed as

$$(P3.4) \quad \min_{\mathbf{F}, t_2, \{t_{3,k}\}} t_2 \quad (21a)$$

$$\text{s.t. } \gamma_k \leq \frac{P_k |\mathbf{w}_k^H \mathbf{h}_k(\mathbf{F})|^2}{\sum_{j=1, j \neq k}^K P_j |\mathbf{w}_k^H \mathbf{h}_j(\mathbf{F})|^2 + \sigma^2}, \quad \forall k \quad (21b)$$

$$\cos(\theta_{\max}) \leq \tilde{\mathbf{f}}_n^T \mathbf{e}_1 \leq 1, \quad \forall n, \quad (21c)$$

(10d), (18b), (18c), (18d).

where constraint (21c) is equivalent to (10c) and restricts RA's zenith angle within $[0, \theta_{\max}]$.

Due to the fractional structure of the SINR expression in constraint (21b), we apply the quadratic transform, yielding

$$f_k(\mathbf{F}, \eta_k) = 2\mathcal{R} \left\{ \eta_k \left(\sqrt{P_k} \mathbf{w}_k^H \mathbf{h}_k(\mathbf{F}) \right) \right\} - |\eta_k|^2 \left(\sum_{j=1, j \neq k}^K P_j |\mathbf{w}_k^H \mathbf{h}_j(\mathbf{F})|^2 + \sigma^2 \right), \quad (22)$$

where η_k is an auxiliary variable introduced by the quadratic transform for each device k . We then iteratively optimize \mathbf{F} and $\{\eta_k\}$ to minimize the objective function in (21a). For a given \mathbf{F} , the optimal auxiliary variable η_k has the following closed-form expression [13]:

$$\eta_k^* = \frac{\sqrt{P_k} \mathbf{w}_k^H \mathbf{h}_k(\mathbf{F})}{\sum_{j=1, j \neq k}^K P_j |\mathbf{w}_k^H \mathbf{h}_j(\mathbf{F})|^2 + \sigma^2}. \quad (23)$$

For fixed η_k^* , the remaining problem with respect to \mathbf{F} is still non-convex due to the nonlinear dependence of $\mathbf{h}_k(\mathbf{F})$ on the RA pointing vectors. To address this issue, we adopt the SCA technique to construct a convex approximation of problem (P3.4). Let $\mathbf{F}^{(i)}$ denote the RA pointing matrix obtained at the i -th iteration. By using the first-order Taylor expansion at $\mathbf{F}^{(i)}$, the term $\mathbf{w}_k^H \mathbf{h}_k(\mathbf{F})$ in (22) can be approximated as

$$\Phi_k^{(i+1)}(\mathbf{F}) \triangleq \mathbf{w}_k^H \mathbf{h}_k(\mathbf{F}^{(i)}) + \sum_{n=1}^N w_{k,n}^* (\mathbf{h}'_{k,n})^T (\tilde{\mathbf{f}}_n - \tilde{\mathbf{f}}_n^{(i)}), \quad (24)$$

where $\mathbf{h}'_{k,n} = \frac{\partial \mathbf{h}_{k,n}(\tilde{\mathbf{f}}_n^{(i)})}{\partial \tilde{\mathbf{f}}_n^{(i)}} = \left(\tilde{\beta}_{k,n} p \left((\tilde{\mathbf{f}}_n^{(i)})^T \tilde{\mathbf{q}}_{k,n} \right)^{p-1} \right) \tilde{\mathbf{q}}_{k,n}$,

with $\tilde{\beta}_{k,n} \triangleq \sqrt{\frac{\kappa_k}{\kappa_k + 1}} \sqrt{L(d_{k,n}) G_0} e^{-j \frac{2\pi}{\lambda} d_{k,n}}$, and $(\cdot)^*$ represents the conjugation operation.

Furthermore, to handle the non-convex constraint in (21b), we construct a quadratic convex upper bound for $u_{k,j}(\mathbf{F}) \triangleq |\mathbf{w}_k^H \mathbf{h}_j(\mathbf{F})|^2$. Let $\nabla u_{k,j}(\tilde{\mathbf{f}}_n)$ and $\nabla^2 u_{k,j}(\tilde{\mathbf{f}}_n)$ denote the gradient vector and Hessian matrix of $u_{k,j}$ with respect to $\tilde{\mathbf{f}}_n$, respectively, whose detailed derivations are provided in Appendix A. Specifically, for a positive real number $\delta_{k,j,n}$ satisfying $\delta_{k,j,n} \mathbf{I}_3 \succeq \nabla^2 u_{k,j}(\tilde{\mathbf{f}}_n)$, whose closed-form expression is given in Appendix B, we have the following quadratic upper bound:

$$u_{k,j}(\tilde{\mathbf{f}}_n) \leq u_{k,j}(\tilde{\mathbf{f}}_n^{(i)}) + \nabla u_{k,j}(\tilde{\mathbf{f}}_n^{(i)})^T (\tilde{\mathbf{f}}_n - \tilde{\mathbf{f}}_n^{(i)}) + \frac{\delta_{k,j,n}}{2} (\tilde{\mathbf{f}}_n - \tilde{\mathbf{f}}_n^{(i)})^T (\tilde{\mathbf{f}}_n - \tilde{\mathbf{f}}_n^{(i)}) \triangleq u_{k,j}^{\text{ub}}(\tilde{\mathbf{f}}_n), \quad (25)$$

which is obtained based on [14, Lemma 12]. Then, the expression (22) can be approximated as

$$f_k(\mathbf{F}, \eta_k) \geq 2\mathcal{R} \left\{ \eta_k^H \left(\sqrt{P_k} \Phi_k^{(i+1)}(\mathbf{F}) \right) \right\} - |\eta_k|^2 \left(\sum_{j=1, j \neq k}^K P_j u_{k,j}^{\text{ub}}(\mathbf{F}) + \sigma^2 \right), \quad (26)$$

where $u_{k,j}^{\text{ub}}(\mathbf{F})$ denotes the constructed convex upper bound applied to RA pointing matrix \mathbf{F} .

C. Overall Algorithm

Algorithm 1 Joint Optimization of $\ell, \mathbf{f}^e, \mathbf{W}, \mathbf{F}$.

Initialize

Set $\mathbf{F}^{(0)} = [\mathbf{e}_1, \dots, \mathbf{e}_1]_{3 \times N}$, threshold $\varepsilon > 0$, and $i=0$.

Compute $\ell^{(0)}$ and $\mathbf{f}^{e(0)}$ by the closed-form solutions in (13) and (15).

repeat

 Compute $\mathbf{W}^{(i+1)}$ by solving problem (P3.3) with given $\ell^{(i)}$, $\mathbf{f}^{e(i)}$, and $\mathbf{F}^{(i)}$.

 Update $\mathbf{F}^{(i+1)}$ by solving problem (P3.4) with given $\ell^{(i)}$, $\mathbf{f}^{e(i)}$, and $\mathbf{W}^{(i+1)}$.

 Calculate $\ell^{(i+1)}$ and $\mathbf{f}^{e(i+1)}$ by the closed-form solution in (13) and (15) with given $\mathbf{W}^{(i+1)}$ and $\mathbf{F}^{(i+1)}$.

 Update $i = i + 1$.

until $\left| \frac{\tau^{\text{comp}(i+1)} - \tau^{\text{comp}(i)}}{\tau^{\text{comp}(i)}} \right| \leq \varepsilon$.

 Integerize $\ell^{(i)}$ by (12).

Output $\ell^{(i)}$, $\mathbf{f}^{e(i)}$, $\mathbf{W}^{(i)}$ and $\mathbf{F}^{(i)}$.

The overall AO algorithm for solving (P1) is summarized in Algorithm 1. Since the objective function τ^{comp} is non-increasing over iterations and lower bounded, the proposed AO algorithm is guaranteed to converge. In each iteration, the computational complexity of solving problem (P2) is $\mathcal{O}\left(I \log_2 \left(\frac{\mu_u - \mu_l}{\epsilon_1} \right) K\right)$, where ϵ_1 is the accuracy of the bisection search and I is the number of inner iterations. The complexity order of problem (P3.3) via the SDR and bisection methods is $\mathcal{O}(N^{4.5} \ln(1/\epsilon_2))$, while that of problem (P3.4) via the SCA method is $\mathcal{O}(N^{3.5} \ln(1/\epsilon_3))$, with ϵ_2 and ϵ_3 being the accuracy thresholds of the bisection search and the SCA method, respectively. Therefore, the overall computational complexity of solving (P1) is $\mathcal{O}(L \cdot (I \log_2 \left(\frac{\mu_u - \mu_l}{\epsilon_1} \right) K + N^{4.5} \ln(1/\epsilon_2) + N^{3.5} \ln(1/\epsilon_3)))$, where L denotes the number of outer AO iterations required for convergence.

IV. Simulation Results

In this section, we present simulation results to verify the performance of our proposed RA-enabled MEC uplink communication system with the proposed AO algorithm. The RA array is centered at the origin, with an inter-antenna spacing of $d = \frac{\lambda}{2}$, $p = 4$, and $\theta_{\max} = \frac{\pi}{6}$. The system operates at 2.4GHz ($\lambda = 0.125$ m) with noise power $\sigma^2 = -60$ dBm. Unless otherwise specified, the simulation parameters are set as follows: $N = 9$, $\zeta_0 = -30$ dB, $\alpha_0 = 2.8$, $\kappa_k = 1, \forall k$, $B = 2$ MHz. We set $L_k = 1000$ Kb, $c_k = 1000$ cycle/bit, and $f_k^l = 6 \times 10^8$ cycle/s for all devices. The offloading transmit powers of all devices are assumed to be identical, i.e., $P_k = P, \forall k$. The devices are assumed to be uniformly distributed over a semicircle centered at the origin with a radius of $r = 40$ m.

For a more comprehensive evaluation of the proposed RA-enabled MEC system (referred to as RA-enabled scheme), the following three schemes are considered: 1) Fixed directional antenna scheme: The deflections of all RAs are fixed as $\tilde{\mathbf{f}}_n = \mathbf{e}_1, \forall n$. 2) Isotropic antenna scheme: The directional gain is set to $G_0 = 1$ with $p = 0$ in (3). 3) Random-orientation scheme: The orientation of each RA is randomly generated within the rotational ranges specified in (10c).

In Fig. 2, we show the latencies of different schemes versus the offloading power P for $K = 4$ and $F_{\max} =$

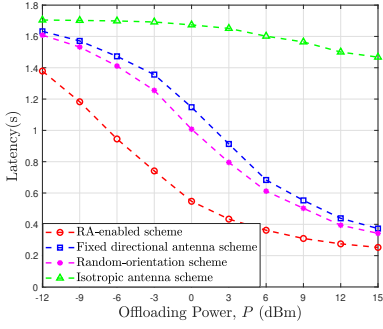


Fig. 2. The maximum computation latency versus offloading power.

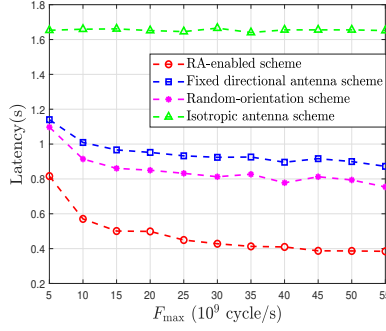


Fig. 3. The maximum computation latency versus the maximum computing capacity.

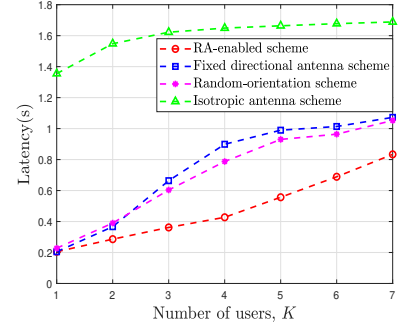


Fig. 4. The maximum computation latency versus number of devices.

30×10^9 cycle/s. It is observed that the latencies of all schemes decrease with increasing offloading power, since a higher power improves the uplink offloading rate. It is worth noting that the performance gap between the proposed RA-enabled scheme and the benchmark schemes becomes less pronounced at very low and high offloading power. At low offloading power, noise dominates the link quality, making the directional gain insufficient to produce noticeable improvement. While at high offloading power, the latency is mainly constrained by the maximum computation capacity, the offloading communication capability is no longer the bottleneck, so the array directional gain provided by RA becomes less critical. Furthermore, the RA-enabled scheme always outperforms the benchmark schemes. This is primarily owing to the ability of RAs to adaptively rotate their boresight directions, which enhances the effective uplink channel gain and increases the offloading rate, thereby reducing the communication latency. In contrast, the isotropic antenna scheme and fixed directional antenna scheme exhibit higher latency due to the absence of directional enhancement, while the random-orientation scheme fails to fully exploit the directional gain owing to its non-optimized antenna orientations.

Fig. 3 illustrates the maximum computation latency versus the maximum computing capacity F_{\max} for $K = 4$ and $P = 3$ dBm. As F_{\max} increases, the latencies of all schemes decrease due to the shortened task execution time at the edge server. When F_{\max} is not high, the computing capability is the bottleneck of latency reduction. But when F_{\max} is high enough, the reduction of the latency becomes small which means that the offloading communication capability plays a dominant role. Therefore, it is not necessary to equip the edge computing node with an extremely powerful computing capability for latency minimization.

Fig. 4 shows the latencies of different schemes versus the number of devices K for $P = 3$ dBm and $F_{\max} = 30 \times 10^9$ cycle/s. It is observed that the RA-enabled scheme consistently outperforms all benchmark schemes, and the latency of each scheme increases with K . This is partially due to the reduced edge computational resources allocated to each device. Moreover, the antenna deflection adjustment becomes more challenging, making it difficult to simultaneously enhance the directional gains for all devices. In addition, when K becomes large, the performance advantage of the RA-enabled scheme over the fixed directional and random-orientation schemes gradually diminishes, since the system becomes increasingly dominated by resource sharing and multi-user competition rather than antenna deflection optimization.

V. Conclusion

In this letter, we investigated an RA-enabled MEC uplink system, where each RA at the BS can flexibly adjust its boresight direction to enhance uplink channel quality for multiple users. By jointly optimizing the MEC server's computing resource allocation, receive beamforming vectors, and the RAs' deflection angles, we developed

an efficient AO framework to minimize the maximum computation latency. Simulation results demonstrated that the proposed RA-enabled MEC design significantly improves latency performance over conventional schemes, highlighting its effectiveness to enable low-latency and high-efficiency computing services in future 6G networks.

Appendix

A. Derivations of $\nabla u_{k,j}(\vec{\mathbf{f}}_n)$ and $\nabla^2 u_{k,j}(\vec{\mathbf{f}}_n)$

For the sake of exposition, we reformulated $u_{k,j}(\mathbf{F})$ as

$$u_{k,j}(\mathbf{F}) = \left| \sum_{n=1}^N w_{k,n}^* \left(\tilde{\beta}_{j,n}(\vec{\mathbf{f}}_n^T \vec{\mathbf{q}}_{j,n})^p + \sqrt{\frac{1}{\kappa_j+1}} \tilde{g}_{j,n} \right) \right|^2, \quad (27)$$

To optimize with respect to a specific $\vec{\mathbf{f}}_n$, we fix the other variables $\vec{\mathbf{f}}_m$ for $m \neq n$ and consider $u_{k,j}$ as a function of $\vec{\mathbf{f}}_n$ only. To facilitate the subsequent derivations, we introduce the following auxiliary variables based on $\vec{\mathbf{f}}_n$: $b_n \triangleq \vec{\mathbf{f}}_n^T \vec{\mathbf{q}}_{j,n}$, $c_n \triangleq w_{k,n}^* \tilde{\beta}_{j,n}$, $\xi_n \triangleq w_{k,n}^* \sqrt{\frac{1}{\kappa_j+1}} \tilde{g}_{j,n}$, and $d_n \triangleq \sum_{m \neq n} w_{k,m}^* \left(\tilde{\beta}_{j,m} b_m^p + \sqrt{\frac{1}{\kappa_j+1}} \tilde{g}_{j,m} \right)$.

Thus, the objective function can be written as $u_{k,j}(\vec{\mathbf{f}}_n) = |d_n + \xi_n + c_n b_n^p|^2$. For convenience, we let $\bar{d}_n \triangleq d_n + \xi_n$ and expand this expression, we obtain:

$$u_{k,j}(\vec{\mathbf{f}}_n) = |\bar{d}_n|^2 + 2\mathcal{R}(\bar{d}_n c_n^* b_n^p) + |c_n|^2 b_n^{2p}. \quad (28)$$

By defining the real coefficients as $A_n = |\bar{d}_n|^2$, $B_n = 2\mathcal{R}(\bar{d}_n c_n^*)$, and $C_n = |c_n|^2$, we arrive at a simplified form:

$$u_{k,j}(\vec{\mathbf{f}}_n) = A_n + B_n b_n^p + C_n b_n^{2p}. \quad (29)$$

Taking derivatives of (29) with respect to b_n , we obtain:

$$\frac{\partial u_{k,j}(\vec{\mathbf{f}}_n)}{\partial b_n} = B_n p b_n^{p-1} + 2C_n p b_n^{2p-1} = p b_n^{p-1} (B_n + 2C_n b_n^p), \quad (30)$$

$$\frac{\partial^2 u_{k,j}(\vec{\mathbf{f}}_n)}{\partial b_n^2} = p(p-1) B_n b_n^{p-2} + 2p(2p-1) C_n b_n^{2p-2}. \quad (31)$$

Applying the chain rule and noting that $\nabla_{\vec{\mathbf{f}}_n} b_n = \vec{\mathbf{q}}_{j,n}$, the gradient vector $\nabla u_{k,j}(\vec{\mathbf{f}}_n)$ and the Hessian matrix $\nabla^2 u_{k,j}(\vec{\mathbf{f}}_n)$ are:

$$\nabla u_{k,j}(\vec{\mathbf{f}}_n) = p b_n^{p-1} (B_n + 2C_n b_n^p) \vec{\mathbf{q}}_{j,n}, \quad (32)$$

$$\nabla^2 u_{k,j}(\vec{\mathbf{f}}_n) = [p(p-1) B_n b_n^{p-2} + 2p(2p-1) C_n b_n^{2p-2}] \vec{\mathbf{q}}_{j,n} \vec{\mathbf{q}}_{j,n}^T. \quad (33)$$

B. Construction of $\delta_{k,j,n}$

Based on the definition of $\nabla^2 u_{k,j}(\vec{\mathbf{f}}_n)$ in Appendix A, we have

$$\|\nabla^2 u_{k,j}(\vec{\mathbf{f}}_n)\|_2 \leq \|\nabla^2 u_{k,j}(\vec{\mathbf{f}}_n)\|_F. \quad (34)$$

Since $\vec{\mathbf{q}}_{j,n}$ is a unit-norm vector, the matrix $\vec{\mathbf{q}}_{j,n} \vec{\mathbf{q}}_{j,n}^T$ is rank-one with a single nonzero eigenvalue equal to 1. Therefore, the spectral norm of $\nabla^2 u_{k,j}(\vec{\mathbf{f}}_n)$ equals the absolute value of its scalar coefficient, which is given by

$$\|\nabla^2 u_{k,j}(\vec{\mathbf{f}}_n)\|_2 = \left| \frac{\partial^2 u_{k,j}(\vec{\mathbf{f}}_n)}{\partial b_n^2} \right|. \quad (35)$$

To ensure a positive semidefinite majorization condition $\delta_{k,j,n} \mathbf{I}_3 \succeq \nabla^2 u_{k,j}(\vec{\mathbf{f}}_n)$, we can directly select $\delta_{k,j,n}$ as

$$\delta_{k,j,n} = |p(p-1) B_n b_n^{p-2} + 2p(2p-1) C_n b_n^{2p-2}|, \quad (36)$$

which guarantees $\delta_{k,j,n} \mathbf{I}_3 \succeq \nabla^2 u_{k,j}(\vec{\mathbf{f}}_n)$, and hence $\delta_{k,j,n} \geq \|\nabla^2 u_{k,j}(\vec{\mathbf{f}}_n)\|_2$. This choice ensures that $\delta_{k,j,n}$ serves as a

valid local Lipschitz constant for the gradient mapping, i.e., $\|\nabla u_{k,j}(\bar{\mathbf{f}}_n) - \nabla u_{k,j}(\bar{\mathbf{f}}_n^{(i)})\| \leq \delta_{k,j,n} \|\bar{\mathbf{f}}_n - \bar{\mathbf{f}}_n^{(i)}\|$.

References

- [1] Y. Mao, C. You, J. Zhang, K. Huang, and K. B. Letaief, "A survey on mobile edge computing: The communication perspective," *IEEE Commun. Surveys Tuts.*, vol. 19, no. 4, pp. 2322–2358, 4th Quart. 2017.
- [2] C. You, K. Huang, H. Chae, and B.-H. Kim, "Energy-efficient resource allocation for mobile-edge computation offloading," *IEEE Trans. Wireless Commun.*, vol. 16, no. 3, pp. 1397–1411, May. 2017.
- [3] Q. Wu, B. Zheng, T. Ma, and R. Zhang, "Modeling and optimization for rotatable antenna enabled wireless communication," in *Proc. IEEE Int. Conf. Commun. (ICC)*, Montreal, Canada, Jun. 2025, pp. 1055–1060.
- [4] B. Zheng, Q. Wu, T. Ma, and R. Zhang, "Rotatable antenna enabled wireless communication: Modeling and optimization," *arXiv preprint arXiv:2501.02595*, 2025.
- [5] B. Zheng, T. Ma, C. You, J. Tang, R. Schober, and R. Zhang, "Rotatable antenna enabled wireless communication and sensing: Opportunities and challenges," *IEEE Wireless Commun.*, pp. 1–8, Oct. 2025.
- [6] L. Zhu, W. Ma, and R. Zhang, "Modeling and performance analysis for movable antenna enabled wireless communications," *IEEE Trans. Wireless Commun.*, vol. 23, no. 6, pp. 6234–6250, Nov. 2024.
- [7] X. Shao, Q. Jiang, and R. Zhang, "6D movable antenna based on user distribution: Modeling and optimization," *IEEE Trans. Wireless Commun.*, vol. 24, no. 1, pp. 355–370, Jan. 2025.
- [8] L. Dai, B. Zheng, Q. Wu, C. You, R. Schober, and R. Zhang, "Rotatable antenna-enabled secure wireless communication," *IEEE Wireless Commun. Lett.*, vol. 14, no. 11, pp. 3440–3444, Jul. 2025.
- [9] C. Zhou, C. You, B. Zheng, X. Shao, and R. Zhang, "Rotatable antennas for integrated sensing and communications," *IEEE Wireless Commun. Lett.*, vol. 14, no. 9, pp. 2838–2842, Jun. 2025.
- [10] Y. Xie, W. Mei, D. Wang, B. Ning, Z. Chen, J. Fang, and W. Guo, "Thz beam squint mitigation via 3D rotatable antennas," in *Proc. IEEE International Conference on Communications Workshops (ICC Workshops)*, Montreal, QC, Canada, Jun. 2025, pp. 26–31.
- [11] X. Xiong, B. Zheng, W. Wu, X. Shao, L. Dai, M.-M. Zhao, and J. Tang, "Efficient channel estimation for rotatable antenna-enabled wireless communication," *IEEE Wireless Commun. Lett.*, vol. 14, no. 11, pp. 3719–3723, Aug. 2025.
- [12] T. Bai, C. Pan, Y. Deng, M. ElKashlan, A. Nallanathan, and L. Hanzo, "Latency minimization for intelligent reflecting surface aided mobile edge computing," *IEEE J. Sel. Areas Commun.*, vol. 38, no. 11, pp. 2666–2682, Jul. 2020.
- [13] K. Shen and W. Yu, "Fractional programming for communication systems—part I: Power control and beamforming," *IEEE Trans. Signal Process.*, vol. 66, no. 10, pp. 2616–2630, May 2018.
- [14] Y. Sun, P. Babu, and D. P. Palomar, "Majorization-minimization algorithms in signal processing, communications, and machine learning," *IEEE Trans. Signal Process.*, vol. 65, no. 3, pp. 794–816, Aug. 2016.